

Roles of OsSOQ1 in photoprotection and fatty acid metabolism of rice

Zhen-Hui Kang (✉ zhkang85@126.com)

Sichuan University of Science & Engineering

Yang Gou

Sichuan University of Science & Engineering

Qi-Rui Deng

Sichuan University of Science & Engineering

Zi-yu Hu

Sichuan University of Science & Engineering

Guan-Rong Li (✉ grli@swu.edu)

Southwest University

Research Article

Keywords: OsSOQ1, thylakoid lumen, non-photochemical quenching (NPQ), fatty acid, OsLCNP

Posted Date: July 1st, 2021

DOI: <https://doi.org/10.21203/rs.3.rs-273323/v1>

License:   This work is licensed under a Creative Commons Attribution 4.0 International License.

[Read Full License](#)

Abstract

Presented here is the function analysis of a homolog of Arabidopsis SOQ1, OsSOQ1 in rice. Homozygous mutants (*ossoq1*) were obtained by CRISPR/Cas9 to knockout *OsSOQ1*. The mutants showed significant lower plant height, tiller number, panicle length, effective panicle, and grain number per panicle compared to the wild-type (WT). Western blot analysis showed that OsSOQ1 is a thylakoid membrane protein, with the thioredoxin-like (Trx-like) domain facing the lumen. Loss of OsSOQ1 did not significantly affect the protein level of photosystem II (PSII) subunits, but down-regulated the content of a non-photochemical quenching (NPQ) player PsbS, resulting in a low NPQ under high light intensity in the mutant. UPLC-MS/MS experiments showed that OsSOQ1 is involved in the fatty acid biosynthesis pathway of rice. The Trx-like domain possessed redox activity *in vitro* as shown by insulin assay; and in the yeast two-hybrid experiment, it was found that the Trx-like domain interacted with the chloroplast lipocalin OsLCNP, which usually binds lipid molecules. These findings revealed that the role of OsSOQ1 is to maintain the photochemical efficiency of PSII under high light intensity and regulate fatty acid metabolism in rice.

1. Introduction

An excess of light absorption will induce excessive excited state of chlorophyll (Chl) molecules. If the energy cannot be transferred out in time through conversion into chemical energy, the energy will be transferred to the surrounding oxygen molecules, resulting in reactive oxygen species (ROS), which will oxidize the photosynthetic membrane, cause its destruction, and inhibit photosynthesis [1, 2]. In order to protect the photosynthetic membrane from light damage, in the long-term evolution process, photosynthesis has developed a series of photoprotective mechanisms to reduce the damage of excess light energy. The heat dissipation is usually detected by non-photochemical quenching (NPQ) of Chl fluorescence, which depends on the the proton gradient (ΔpH) across thylakoid membrane and the xanthophyll cycle [3, 4].

There are five components of NPQ in total, defined as q_E , q_Z , q_T , q_I and q_H respectively. Each component has its own induction and relaxation kinetics, and each has its own known dependable factors [5]. The major component of NPQ is q_E , which depends on three factors ΔpH , PsbS, and zeaxanthin [6]. The Arabidopsis deficient in PsbS and zeaxanthin is termed as *npq2* and *npq4* respectively. The *npq2* and *npq4* are xanthophyll cycle mutants, closely associated with reversible conversion of violaxanthin to zeaxanthin [7]. The *npq 4*, deficient of proton sensor protein PsbS, provides a quenching site of q_E [8]. Zeaxanthin-dependent quenching is called q_Z , requires the formation of zeaxanthin but not ΔpH [9]. q_T depending on STN7 kinase is responsible for the state transition between PSI and PSII, due to the necessity that the phosphorylated antenna proteins need to move away from PSII [10, 11]. q_I or photoinhibitory quenching is a slow-relaxing process, which accounts for the photoinhibitory quenching of PSII reaction centers [12]. q_H accounts for a slowly relaxing process in the peripheral antenna of PSII [13]. In addition, there is also a special NPQ component called q_M , which accounts for the fluorescence parameter due to chloroplast movements [14].

The thylakoid lumen is a narrow continuous space enclosed by thylakoid membrane. The luminal proteins in higher plants have been revealed to have multiple functions for PSII [15]. PSII could easily be photodamaged by high light intensity. The damaged PSII is disintegrated from grana thylakoid and moved to the stroma lamellae and rearranged there. During this process, PSII core protein D1 are degraded by luminal and stroma deg/Fst protease and re-synthesized [16]. The luminal peripheral protein of PSII, PsbO is phosphorylated by a nucleoside diphosphate kinase NDPK3 and is dephosphorylated by luminal acid phosphatase tlp18.3, which is involved in the phosphorylation signaling of PSII assembly [17, 18]. After reassembly, the intact PSII complexes return to the grana thylakoid.

Several luminal enzymes have activity only in light when the pH of lumen is acidic due to the formation of ΔpH [19]. Through noncyclic electron transport chain, electrons are finally transferred to NADP^+ , the final electron acceptor, which is used for carbon fixation. With regard to the assembly of luminal proteins for the photosystem complex, the electrons needed was transferred from chloroplast stroma thioredoxins (Trxs). HCF164 has been shown to be an electron donor in the lumen [20]. HCF164 was firstly identified as a factor being involved in the assembly of Cyt b_6/f complex, through reducing FeS protein and Cyt b_6 . PSI-N was another target of HCF164 because of its Trx domain.

The suppressor of quenching 1 (SOQ1) in Arabidopsis had been introduced as a luminal protein maintaining the efficiency of light harvesting [12]. The SOQ1 protein is a negative regulator of qH, which is independent of zeaxanthin, PsbS, ΔpH , STN7, and D1 repairment. The SOQ1 spans the thylakoid membrane with a molecular weight (MW) of 104 kDa [21]. The stroma-exposed region of SOQ1 contains a haloacid dehalogenase-like hydrolase (HAD) domain, and the lumen-exposed region contains a thioredoxin-like (Trx-like) and β -propeller NHL domain [12]. It is the luminal Trx-like not the stromal domain that is required to suppress qH [22]. The formation of qH is prevented by SOQ1 reducing luminal or lumen-exposed target proteins [23]. Possible mechanism is that one or more quenching site(s) is formed in the peripheral and/or proximal PSII antenna in the absence of SOQ1, which decreases the lifetime of excited-state Chl [24]. However, its reduced activity and target proteins remains unidentified.

The SOQ1 was originally characterized in a screening of quenching suppressor(s) in *npq4* background, a qE-deficient line that cannot dissipate excess light energy absorbed [3]. The *npq4* was mutagenized again to produce *soq1 npq4* double mutant, which shows high and slowly relaxing NPQ [12]. Several qH players had been gradually characterized through this screening strategy. By using *soq1 npq4* as the background material, two more players involved in photoprotection qH, chl *a* oxygenase (CAO), responsible for the conversion of Chl *a* to Chl *b*, and a luminal lipocalin (LCNP) was identified [21]. In addition, ROQH1, an atypical short chain dehydrogenase/reductase is required to turn off qH, which is a sustained form of antenna quenching, and is induced by high light intensity and cold stress [23]. The *soq1 roqh1* double mutant displays a low fluorescence phenotype, indicative of possible constitutive NPQ. It has been pointed out lately that novel molecular players (suppressors and enhancers) involved in photoprotection qH could be identified through conducting *soq1 npq4* double mutant and Chl fluorescence imaging [22]. In addition, the SOQ1 was shown as a downstream factor of the chloroplast Trx system leading by the NADPH-dependent Trx reductase C (NTRC), which modulates photosynthesis depending on light intensity

and leaf age [25]. SOQ1 is supposed to accept electrons from NTRC. If the amount of NTRC enhanced, it would persistently activate SOQ1, and finally repressed the qH-type NPQ.

It has been previously reported that a thylakoid lumenal protein, OsTLP27, is required for accumulation of photosynthetic proteins in rice [26]. However, characterization of the lumenal proteins still remains largely insufficient in rice, especially the downstream/target proteins and the role in metabolism of OsSOQ1. Here, the function analysis of a homolog of Arabidopsis SOQ1, OsSOQ1, also a multi-domain protein in rice, is presented. It has been shown that *OsSOQ1* is related to the drought response in rice [27]. Homozygous mutants (*ossoq1*) were obtained by CRISPR/Cas9 to knockout *OsSOQ1*. The mutants showed significant lower plant height, tiller number, panicle length, effective panicle, and grain number per panicle relative to the WT plants. Western blot analysis showed that OsSOQ1 is a thylakoid membrane protein, with the Trx-like domain facing the lumen. Deficient in OsSOQ1 did not affect the protein level of PSII subunits, but down-regulated the level of a NPQ player PsbS, resulting in a low NPQ under high light intensity in the mutants. UPLC-MS/MS experiments showed that OsSOQ1 is involved in fatty acid metabolism in leaves. The Trx-like domain exhibited redox activity *in vitro* as shown by insulin assay; and in the yeast two-hybrid experiment, it was found that the Trx-like domain interacts with the chloroplast lipocalin OsLCNP, which usually transports lipid molecules. These critical findings revealed that the role of OsSOQ1 is to maintain the photochemical efficiency of PSII under high light intensity and regulate the metabolism of fatty acid in rice.

2. Materials And Methods

2.1 Rice and cultivation

Oryza sativa L. *japonica* cv., zhonghua11(zh11), and wild-type (WT) were used as transformation recipients for the construction of transgenic knockout plants in this study. The rice plants were pot cultivated and grown in a greenhouse at 30 °C and 70% humidity under a photoperiod of 16 h light/8 h dark.

2.2 CRISPR/Cas9 knockout and genetic transformation

The CRISPR/Cas9 gene editing system was used to generate transgenic *OsSOQ1* knockout rice plants. The small guide RNA (sgRNA)-Cas9 expression vectors were constructed as previously described [28]. The designed sgRNA sequence (GGGTAGCGCCGGGGCCTGG) was inserted between the promoter and the sgRNA scaffold by recombination reaction. The CRISPR vectors were introduced into zh11 callus by *Agrobacterium* EHA109-mediated transformation as reported by [29]. To detect the presence of the desired mutations in the transgenic rice plants, *OsSOQ1* was PCR amplified by *OsSOQ1*-specific primers with genomic DNA template, and the product sequenced. The sequence chromatograms were aligned with the WT control plants generated from non-transgenic callus at the same age. The homozygous mutants were selected for further experiments. The WT and transgenic seedlings were transferred into growth chamber in a greenhouse and grown under a photoperiod of 16 light/8 h dark with 120 $\mu\text{mol m}^{-2}$

s^{-1} light intensity. For agronomic trait analysis, samples from WT and transgenic plants were harvested after the heading stage.

2.3 Vector construction

Total RNA of rice leaves was extracted and the cDNA was synthesized by RT-PCR. The Trx-like domain fragment of OsSOQ1 was amplified by PCR, sequence confirmed, and used for constructing yeast two-hybrid plasmid. The primers used in this study were listed in supplements (Table S1).

2.4 Protein preparation in the chloroplast subtractions

Protein isolation of chloroplast subtractions was mainly conducted as described by [30]. In brief, leaf tissue suspension was filtered by nylon cloth after homogenization and then centrifuged to remove the cell debris. Intact chloroplasts were recovered through Percoll density gradient centrifugation. The chloroplasts were firstly subject to hypotonic break, then the chloroplast envelope, stroma and intact thylakoid membranes were recovered by sucrose density gradient centrifugation. The thylakoid membranes were hypotonic break again, then sonicated to prepare soluble lumenal proteins and pure thylakoid membranes. Proteins in chloroplast stroma and thylakoid lumen were both concentrated and purified by ultrafiltration. To solubilize the proteins anchoring in the chloroplast envelope and thylakoid membranes, a final concentration of 1% Triton X-100 was added. Chloroplast compartment marker proteins were purchased from Huada (China) and Agerisera (Sweden).

2.5 Measure of Chl fluorescence

Chl fluorescence was measured by using a FMS-1 portable fluorometer (Hansatech, UK). Prior to measurement, plants were adapted in dark for over 30 min to make sure that PSII reaction center was fully opened. The minimum fluorescence yield (F_0) was measured with detection light. To measure the maximum fluorescence yield (F_m), a saturating pulse of white light was applied. The maximum photochemical efficiency of PSII in dark was calculated as $F_v/F_m = (F_m - F_0)/F_m$. To measure the maximum fluorescence in any light-adapted state (F_m'), the leaves were irradiated usually by an un-saturating actinic light with an illumination period of within 3 min. Then a saturated pulse of white light was applied to measure F_m' and then the minimal fluorescence in any light-adapted state (F_0') with a far-red light. The NPQ was calculated as $F_m/F_m' - 1$. All measurements were performed with six biological replicates at 25°C.

2.6 Recombinant protein preparation of Trx-like domain and Insulin assay

Specific primers with restrict sites were synthesized according to the sequences of the Trx-like domain. The recombinant plasmids were transformed into *E. coli* BL21 (DE3) strains. *E. coli* lysates were prepared to purify His-tagged proteins under denaturing conditions of 8 M urea in Ni-NTA column (Bio-Rad, USA). Unspecific proteins were further removed by FPLC (AKTA, USA). The protein concentration was determined by Lowry method following the manufacturer's protocol. Five micromole of recombinant

protein was used for activity assay. For redox activity detection of the Trx-like domain, insulin assay was conducted as described by [31].

2.7 Yeast two-hybrid assay

In this assay, pGBKT7-OsSOQ1 recombinant vector harboring the Trx-like domain was used to screen the rice cDNA library as the bait plasmid, while the pGADT7 was used to construct the prey plasmid. Positive clones were verified by sequencing to identify interacting proteins. Yeast co-transformation was performed to further confirm the interaction between Trx-like domain of OsSOQ1 and the candidate protein by using a LiAc/PEG method as described in Yeast Protocols Handbook (Clontech). The pGBK-T53 and pGAD-T7 was used as a negative and positive control respectively. After transformation, yeast cells were plated on selected SD medium (-Leu/-Trp/-His/-Ade/-X-gal) and cultured for 3 d at 30 °C.

2.8 Western blot and protease protection assay

Leaf total protein was extracted by protein extraction kit (Shenggong, China) as instructed. After protein pellet is resolved in 6 M guanidine hydrochloride, the protein concentration was determined by the Bradford method. For western blot analysis, total protein was separated in SDS-PAGE gels and then transferred to the PVDF membrane. The immunoblot experiments was conducted by the standard procedure [32]. Finally, signals were detected with the horseradish peroxidase (HRP)-conjugated chemiluminescence method. To perform the protease protection assay, the intact thylakoid membranes was sonicated and then incubated on ice for 30 min with 20 $\mu\text{g } \mu\text{L}^{-1}$ thermolysin (Th), then the membrane proteins were separated by SDS-PAGE and immunodetected with specific anti-OsSOQ1 antibody. The antibody against to actin was used as a protein loading control.

2.9 Protein expression pattern of OsSOQ1

For OsSOQ1 protein expression at different ages, rice leaves of 15-d-old, 8-week-old and 15-week-old WT plants were harvested. For tissue expression level analysis, total protein in the stem, leaf blade, leaf sheaths and young glume at the heading stage were extracted. The 15-d-old WT seedlings grown in 1/2 MS liquid medium were subject to high light intensity treatment for 2 h or cold stress treatment at 6°C for 6 h, or drought stress treatment with 20% PEG6000 respectively for 3 d.

2.10 Quantitative reverse transcription-PCR (qRT-PCR)

Total RNA was extracted from leaves with Trizol reagent. First-strand cDNA was synthesized with 1 μg of total RNA. qRT-PCR was performed in a CFX96 thermocycler (Bio-rad. USA). *Actin* was used as an internal control. The relative expression level of the gene were calculated as the $2^{-\Delta\Delta\text{CT}}$ method.

2.11 Antibody preparation

Epitopes of OsSOQ1 was predicted online and its polyclonal antibodies was generated by Wenyuange Company Ltd. (Shanghai, China) against synthetic polypeptide antigen EFYEENKLLQNSS (540–552 aa).

2.12 Detection of thylakoid membrane lipids

Leaves of 15-d-old seedlings were homogenized in ice-cold blender and centrifuged to prepare the total lipid phase. For measurements of monogalactosyl-diacylglycerol (MGDG) and digalactosyl-diacylglycerol (DGDG), phosphatidylglycerol (PG), sulfoquinovosyl diacylglycerol (SQDG), and phosphatidylethanolamine (PE), lipid samples were extracted by hexane, and fatty acid methyl esters were separated by two-dimensional TLC and detected by enzyme linked immunosorbent assay (ELISA) kits following the manufacturer's protocols. The optical density (OD) value at 450 nm was measured with a microplate, and the concentration of the five lipids was calculated by the standard curve. All the tests were performed at Kechuang Quality Analysis Ltd. (Qingdao, China).

2.13 Measurement of pigments

Chl content was measured as described by [33]. Leaves from two-leaf seedlings were ground in liquid N₂. Total pigments was extracted with a mixture of ethanol, acetone and water (4.5:4.5:1, v/v/v). Absorption values at 663, 645 and 470 nm were used to calculate the Chl and carotenoid (Car) content. Total Chl is calculated as described by [34]. All the measurements were carried out with six biological replicates at 25°C.

2.14 Ultra performance liquid chromatography/tandem mass spectrometry (UPLC-MS/MS)

Tissues (100 mg) were grounded with liquid N₂ and the homogenate was re-suspended with pre-chilled 80% methanol and 0.1% formic acid. Prior to be injected into the UPLC-MS/MS system, the samples were centrifuged at 20000 *g*, 4 °C for 10 min. UPLC-MS/MS analyses were performed using a Vanquish UHPLC system (Thermo Fisher) coupled with an Orbitrap Q Exactive series mass spectrometer. Samples were injected into a Hyperil Gold column using a 16-min linear gradient at a flow rate of 0.2 mL min⁻¹. The mass spectrometer was operated in positive/negative polarity mode with spray voltage of 3.2 kV, capillary temperature of 320 °C, sheath gas flow rate of 35 arb and aux gas flow rate of 10 arb. The raw data files generated by UHPLC-MS/MS were processed using the Compound Discoverer 3.1 to perform peak alignment, peak picking, and quantitation for each metabolite. The normalized data was used to predict the molecular formula based on additive ions, molecular ion peaks and fragment ions. And then peaks were matched with the mzCloud (<https://www.mzcloud.org/>), mzVault and MassList database to obtain the accurate qualitative and relative quantitative results. These metabolites were annotated using the KEGG database (<http://www.genome.jp/kegg/>), HMDB database (<http://www.hmdb.ca/>) and Lipidmaps database (<http://www.lipidmaps.org/>).

2.15 Statistical Analysis

All the experiments were repeated at least three biological replicates. SPSS software (version 13) and Student's *t*-test was used for statistical analysis and significant difference analysis respectively.

2.16 Accession Numbers

Sequence data from this article can be found in the GenBank/EMBL data libraries under the following accession: OsSOQ1 (Os03g0311300), OsLCNP (XM_015780451).

3. Results

3.1 OsSOQ1 is a positive regulator in the development of rice

In order to study the physiological role of OsSOQ1 in rice, the CRISPR/Cas9 knockout plasmid harboring specific sgRNA of *OsSOQ1* was constructed and transformed into rice zh11 callus. After screening by antibiotic resistance, twenty knockout mutant lines were finally obtained. After high-throughput sequencing of these transgenic plants, it was found that six lines were screened as positive mutants, with two of them being homozygous mutants (*ossoq1*). After germination of the homozygous seeds on 1/2 MS medium, seedlings were transplanted in soil and grown under natural conditions. The phenotype was observed throughout the growth period.

As compared with WT, the *ossoq1* shows a lower plant height phenotype, indicating that the development of mutant plants was indeed influenced by loss of OsSOQ1 (Fig. 1a). To further determine whether the phenotype of the mutant is caused by a genetic mutation in OsSOQ1 gene, genomic DNA of WT and mutant plants were extracted and subject to sequencing. The obtained sequences were aligned by Snapgene software. A deletion of a base T at position 381 of the *OsSOQ1* gene was identified, resulting in a premature-termination in translation of the protein, a polypeptide of 132 aa (Fig. 1b). In order to confirm the deficiency of the normal OsSOQ1 protein in the mutants at translation level, a specific anti-rabbit polyclonal antibody against OsSOQ1 was raised and used to detect the protein level of OsSOQ1 in WT and mutant leaves. A dense protein band around 110 kDa was detected in WT, but not in three mutant lines (Fig. 1c). The antibody also detected a few nonspecific bands in both WT and mutant leaves, but their pattern was nearly identical, showing that the antibody had successfully detected the positive band, and the mutants did not express the OsSOQ1 protein. These results indicated that OsSOQ1 was indeed knocked out in the mutant plants. Also studied are the agronomic traits and pigment contents of the WT and mutant rice. It was found that the plant height, tiller number, panicle length, effective panicle, grain number per panicle of *ossoq1* was significant lower than those of WT (Fig. 1d-h). However, there is no significant difference with respect to the 1000-grain weight between *ossoq1* and WT (Fig. 1i). The Chl and carotenoid (Car) content in mutant leaves was largely unaffected as compared with those in WT (Fig. 1j-k). These results showed that function loss of OsSOQ1 has a general negative impact on the development of rice.

3.2 OsSOQ1 is a thylakoid membrane protein with Trx-like domain localizing in the lumen

Next, bioinformatics and experimental operation were used to study the localization of OsSOQ1 protein. By searching for the *Os03g0311300* encoding OsSOQ1 in the Plant Proteome Database (PPDB,

<http://ppdb.tc.cornell.edu/dbsearch/searchacc.aspx>), it was found that OsSOQ1 has a chloroplast transit peptide (cTP), a HAD domain (89–256 aa) and a Trx-like domain (297–540 aa). In addition, TopPred software prediction revealed OsSOQ1 contains a transmembrane segment between the HAD and Trx-like domain (304–326 aa), indicating that OsSOQ1 is most likely a chloroplast protein.

The localization of OsSOQ1 in chloroplast was then investigated by use of chloroplast marker proteins [Tic40 for the envelope, RbcL for the stroma, PsbS for the thylakoid membrane and violaxanthin de-epoxidase (VDE) for the thylakoid lumen]. Through Percoll and sucrose density gradient centrifugation, a series of chloroplast subfractions were prepared, and the subfractions were subjected to SDS-PAGE and blotted either by markers or anti-OsSOQ1 antibody. It was revealed that each chloroplast subfraction was immunoblotted by its corresponding marker protein antibodies as expected, while signals visualized by anti-OsSOQ1 antibody could only be detected in the thylakoid membrane (Fig. 2a), indicating that OsSOQ1 is anchored in thylakoid membrane.

Given that OsSOQ1 was a thylakoid membrane protein with a potential transmembrane domain, then protease protection assays for OsSOQ1 were performed. After treatment with Th, the thylakoid membrane proteins were subject to western blot analysis. A specific band is immuno-detected by OsSOQ1 specific antibody at the original position of OsSOQ1 protein in the untreated control (Fig. 2b, upper panel). However, after treatment with Th, there was a shift at lower position for the OsSOQ1 band (red arrowhead indicated), with a lower level at the original position, perhaps due to the incomplete proteolysis of the original OsSOQ1 protein. It could be seen that the major part of OsSOQ1 was localized at the inner periphery of the thylakoid membrane (luminal side). If the thylakoid membrane was sonicated, it would be broken only to form a lipid bilayer and released the soluble luminal proteins. Thus, it will be unable to protect the inner periphery proteins at the luminal side from Th degradation. When sonicated thylakoid samples were treated with Th, the OsSOQ1 band was merely detectable with OsSOQ1 antibody (Fig. 2b, lower panel).

3.3 OsSOQ1 is involved in the NPQ possibly by regulating PsbS

It has been reported that drought will induce the expression of *OsSOQ1*. Thus the protein expression pattern of OsSOQ1 under stress conditions were studied. Results showed that the expression level of OsSOQ1 could be induced by high light intensity, cold and drought stresses, to varying degrees (Fig. 3a). The drought response of OsSOQ1 is consistent with the previous study [27]. Also studied was the protein level of OsSOQ1 at different developmental stages and in different aboveground tissues in rice. The protein of OsSOQ1 could be detected in leaves at seeding, tillering and mature stage (Fig. 3b). The tissue expression pattern showed that except for the stem, the OsSOQ1 was expressed in all the green tissues, including the young glume, leaf sheaths, and leaf blade (Fig. 3c).

The Chl fluorescence parameters were measured for the WT and mutants. As compared with WT, the F_v/F_m of *ossoq1* was not disturbed by loss of OsSOQ1, meaning that there was not a direct connection between PSII and OsSOQ1 (Fig. 3d). To understand whether the knockout of OsSOQ1 had an impact on

other photosynthetic proteins, the accumulation of OspsbC (CP43 protein of PSII), OspetB (cytochrome b_6), ATP synthase, RbcL and RbcS in the transgenic and WT plants under normal growth light were assayed by western blot analysis. It was observed that the expression of OspsbC, OspetB, ATP synthase, RbcL and RbcS were largely unaffected in the absence of OsSOQ1 (Fig. 3e), indicating that OsSOQ1 did not affect the accumulation of photosynthetic proteins under normal light.

The NPQ is usually induced in higher plants when absorbing excessive light. The WT and mutant plants were treated with high light intensity for 10 min, and both showed a NPQ induction (Fig. 3f). However, the NPQ in the mutants showed a lower induction and slower relaxation process when dark adapted for 10 min. It could be seen that *ossoq1* had a lower potential for dissipating excessive light energy.

PsbS is necessary for photoprotective thermal dissipation of excess absorbed light energy in plants. VDE determines the concentration of zeaxanthin in chloroplasts, which induces the dissipation of excitation energy in the Chl of the light-harvesting protein complex of PSII. The protein level of PsbS detected was significantly decreased, while the level of VDE, basically unaffected in the mutants compared with the WT plants (Fig. 3g), suggesting that the knockout of OsSOQ1 leading to a low NPQ in *ossoq1* is probably due to the downregulated PsbS. These results showed that OsSOQ1 protected the thylakoid membrane from stress damage in rice.

3.4 OsSOQ1 interacts with chloroplastic lipocalin OsLCNP and is involved in the metabolism of fatty acids.

OsSOQ1 was found to contain a HAD and Trx-like domain through bioinformatics analysis of protein structure. In order to verify whether OsSOQ1 reduces the activity of other target proteins in the thylakoid lumen through redox regulation, it is necessary to detect whether the Trx-like domain has reducing activity. The DNA fragment of Trx-like domain was amplified by PCR and inserted into the *pet28a* prokaryotic expression vector. After the recombinant protein was expressed and purified, as shown in Fig. 4a (inbox). The recombinant protein is tested by insulin assay to determine the degree of insulin reduction to determine its reducing activity. It was found that the Trx-like domain of the recombinant protein began to reduce the substrate after 35 min (Fig. 4a), confirmed its reducing activity.

In order to elucidate the regulatory role and the relevant signaling pathway of OsSOQ1 at protein interaction level, yeast two-hybrid experiments were performed to screen its interacting proteins. By screening the rice cDNA library using pGBKT7-OsSOQ1 as a bait, a few interacting proteins with OsSOQ1 were identified through sequencing, among which more attention was paid to a lipocalin termed OsLCNP. LCNP plays a role in abiotic stress and in protecting against lipid peroxidation. In Arabidopsis, LCNP is required for qH to occur. Their interaction was further determined by yeast co-transformation *in vitro*. The yeast strain harboring both OsSOQ1 and OsLCNP vectors could grow on the QDO/X/A (SD/-Leu/-Trp/-His/-Ade) medium (Fig. 4b), which means that the OsSOQ1 interacts with OsLCNP *in vitro*. Yeast strains containing Y2Hgold (pGBKT7-53) and Y187 (pGADT7-T) were used as a positive control, whose strain substantially grow on the QDO/X/A medium, while the negative control Y2Hgold (pGBKT7-Lam) and Y187 (pGADT7-T) cannot grow on selective medium. Finally, the expression of *OsLCNP* in *ossoq1* by qRT-

PCR was studied. It was shown that the expression of *OsLCNP* was substantially downregulated in *ossoq1* in contrast to WT (Fig. 4c).

3.5 Metabolites in fatty acid biosynthetic pathway were disturbed in *ossoq1*

In order to determine the influence of OsSOQ1 mutation on the biosynthesis of metabolites in rice, the metabolism of *ossoq1* was studied by UPLC-MS/MS. A total of 529 metabolites were detected in the leaves of WT and *ossoq1*, among which, a total of 176 metabolites showed significant differential accumulation in *ossoq1* relative to WT, with 72 metabolites upregulated and 104 downregulated in *ossoq1*. These differentially accumulated metabolites including unsaturated fatty acids, benzoxazinoid, linoleic acid, monoterpenoid, phenylalanine, carotenoid, flavonoid and phenylalanine were listed in KEGG enrichment (Fig. S1 and S2). Interestingly, the biosynthesis of unsaturated fatty acids was both enriched in positive and negative polarity mode in UPLC-MS/MS analysis. Metabolite quantitative results were listed in Supplemental Tables 2 and 3.

The thylakoid membrane mainly contains two major lipids monogalactosyl-diacylglycerol (MGDG), digalactosyl-diacylglycerol (DGDG), and three minor lipids sulfoquinovosyldiacylglycerol (SQDG), phosphatidylglycerol (PG), and phosphatidylethanolamine (PE). These five lipids were detected by UPLC-MS/MS in leaves of WT and *ossoq1* and compared (Supplemental Tables 2 and 3). To further ascertain whether OsSOQ1 has an impact on the composition of thylakoid membrane lipids, the contents of the five lipids in WT and mutant leaves at mature stage were assayed by ELISA. These results revealed that under normal growth light intensity the content of MGDG, SQDG and PG in the mutant was significantly higher than in WT (Fig. 5a-c). However, DGDG was significantly downregulated in *ossoq1* in contrast to WT (Fig. 5d), and PE was the only one not significantly affected in the mutant (Fig. 5e). Surprisingly, when the WT and *ossoq1* plants were treated under high light intensity for 2 h, this situation remained unchanged (Fig. 5a-e). These results not only verified the reliability of the UPLC-MS/MS results, but also demonstrated that OsSOQ1 is involved in the composition of the thylakoid membrane lipids, and is independent of high light intensity.

4. Discussion

To the best of our knowledge, this represents the first report describing the biofunctional characterization of a thylakoid luminal protein gene, *OsSOQ1*, and its roles in the photoprotection and fatty acid metabolism in rice.

4.1 OsSOQ1 maintains the photochemical efficiency of PSII under high light intensity in rice.

This study provided evidence that the Trx-like domain of OsSOQ1 is located in the thylakoid lumen (Fig. 2b) and has redox activity (Fig. 4a). It was suggested that OsSOQ1 might be involved in the redox regulation in the thylakoid lumen. Except for the chloroplast envelope, the other chloroplast subfractions

contain the target proteins of Trx, so that the disulfide bonds of many thylakoid lumenal proteins are redox-regulated [35]. From this point of view, the role of thylakoid lumenal redox regulation of many biological activities (such as protein transport, folding and function) could not be underestimated [36]. Redox regulation controls the activity and function of many thylakoid lumenal proteins, enable them to play an indispensable role in the maintenance of photosynthetic efficiency such as by preventing the singlet oxygen stress [37].

OsLCNP was identified as an interacting protein of OsSOQ1 through screening of yeast two-hybrid experiments (Fig. 4b). In Arabidopsis, LCNP is a plastid lipocalin and required for qH. Lipocalin has an enzymatic activity and can bind small hydrophobic molecules such as fatty acids [38]. qH is PsbS- and Δ pH-independent quenching type, which requires LCNP and is repressed by SOQ1 [21]. However, the identity of the putative ligand or substrate of LCNP is still unknown. LCNP localized in the lumen contains six conserved cysteine residues and is a soluble protein of 29 kD [21]. Under high light intensity, the redox activity of OsSOQ1 might reduce the disulfide to activate OsLCNP, as qH functions under stress conditions such as high light intensity. So, it is speculated that similar to SOQ1 in Arabidopsis, the OsSOQ1 in rice also is a member being involved in the qH photoprotection mechanism as clear evidence of physical interaction between OsSOQ1 and OsLCNP had been provided in this study. Moreover, it is proposed that the OsSOQ1 together with OsLCNP perform the function to protect the photosynthetic apparatus and maintain photochemical efficiency in plants. Further research could focus on identifying the putative ligand or substrate of OsLCNP.

There are three usages of the light energy absorbed by the photosynthetic machinery in higher plants: the photochemical reaction of the Chl molecules in the reaction center, which leads to charge separation and subsequent electron transport, the dissipation in the form of heat, and the Chl fluorescence [39, 40]. Both the photochemical reaction and heat dissipation can cause the decrease of Chl fluorescence emission, termed as Chl fluorescence quenching [41, 42]. The fluorescence quenching of Chl caused by photochemical reaction is called photochemical quenching, and the fluorescence quenching caused by heat dissipation is called NPQ [43]. The level of NPQ reflects the magnitude of heat dissipation [44]. qE is the fast phase of NPQ dissipating excess absorbed light energy as heat [45]. Under high light intensity, the acidification of the thylakoid lumen promotes the protonation of PsbS protein, which senses the change of the thylakoid lumenal pH and activates VDE, which then converts violaxanthin into zeaxanthin [46]. A few photosystem subunits in *ossoq1* is largely unaffected (Fig. 3e), indicating that loss of OsSOQ1 did not affect the assembly of PSII. Two NPQ related proteins, VDE and PsbS, were also detected by western blot in WT and *ossoq1*. PsbS is a quenching site of qE [12]. The protein level of VDE in mutants was relatively similar to that in WT plants, while the level of PsbS was down-regulated by 30% (Fig. 3g), indicating that high NPQ might operate in the mutant plants. Under high light intensity stress, NPQ will increase, which is conducive to the dissipation of excess light energy and has a protective role. However, if in this case, NPQ does not function normally, excess light energy will accumulate, and then result in photoinhibition or even photodamage [47]. This speculation was reconfirmed in the NPQ kinetics experiments (Fig. 3f). Unlike the SOQ1 in Arabidopsis which is only a negative regulator of qH, however,

OsSOQ1 in rice is also involved in the qE photoprotection depending on PsbS in rice as revealed in this study.

4.2 The OsSOQ1 is involved in the regulation of fatty acid metabolism

Besides being a photosynthetic organelle, the chloroplast is also a major synthetic site for fatty acids in plants. In part, glycolipids are synthesized through the prokaryotic synthesis pathway in the chloroplast envelope [48]. In this study, the evidence that the biosynthesis of fatty acid had been affected in *ossoq1* was provided (Fig. 5). Trans-9-octadecenoic acid was one of the downregulated metabolites in mutant as compared with that in WT (Supplemental table 2 and 3). As a plastid lipocalin, OsLCNP was found to interact with OsSOQ1 (Fig. 4b), whose function was supposed to bind fatty acids. Moreover, the expression level of *OsLCNP* was significant down-regulated in *ossoq1* in contrast to that in WT. Thus, it could be speculated that the absence of Trx-like domain of OsSOQ1 could not reduce to active OsLCNP, cause a block in the transferring of lipids, and finally result in a stunted development of rice.

In summary, it is found in this study that OsSOQ1 in rice, besides plays a role in photoprotection, also in the biosynthesis of fatty acids. The results provided in this research deepens and widens our understanding on the function of OsSOQ1 in rice. Further studies should be particularly focused on manipulating OsSOQ1 through gene overexpression to improve the photosynthetic capacity.

List Of Abbreviations

Chl, chlorophyll; ROS, reactive oxygen species; ΔpH , the proton gradient; NPQ, non-photochemical quenching; PSI, photosystem I; PSII, photosystem II; NDPK3, nucleoside diphosphate kinase; Trx, thioredoxin; SOQ1, suppressor of quenching 1; MW, molecular weight; HAD, haloacid dehalogenase-like hydrolase; CAO, Chlide a oxygenase; NTRC, NADPH-dependent TRX reductase C; sgRNA, single guide RNA; F_0 , minimum fluorescence yield; F_m , maximum fluorescence yield; F_m' , maximum fluorescence in any light-adapted state; F_0' , minimal fluorescence in any light-adapted state; HRP, horseradish peroxidase; Car, carotenoid; Ultra performance liquid chromatography/tandem mass spectrometry (UPLC-MS/MS); MGDG, monogalactosyl-diacylglycerol; DGDG, digalactosyl-diacylglycerol; PC, phosphatidylcholine; PE, phosphatidylethanolamine; PG, phosphatidylglycerol; PI, phosphatidylinositol; SQDG, sulfoquinovosyldiacylglycerol. OD, optical density; VDE violaxanthin de-epoxidase; Th, thermolysin

Declarations

Ethics approval and consent to participate

Not applicable

Consent for publication

Not applicable

Availability of data and materials

The original contributions presented in the study are included in the Supplementary Material, further inquiries can be directed to the corresponding author.

Competing interests

The authors declare no conflict of interest. We have no financial and personal relationships with other people or organizations that can inappropriately influence our work. There is no professional or other personal interest of any nature or kind in any product, service and/or company that could be construed as influencing the position presented in, or the manuscript entitled.

Funding

This work was supported by National Science Foundation of China (31601291), Project of Talent Introduction in Sichuan University of Science and Engineering (2016RCL14) and Project of Department of Sichuan Science and Technology (2020YFN0023)

Authors' Contributions

Zhen-Hui Kang supervised the project and designed the experiments. Qi-Rui Deng and Zi-Yu Hu helped with literature searching. Yang Gou performed the experiments, analyzed and interpreted the data. Zhen-Hui Kang and Guan-Rong Li wrote the paper.

Acknowledgments

We appreciated Miss. Tong Qin from Sichuan University for helping analyze the data in the manuscript.

References

1. Earles JM, Theroux-Rancourt G, Gilbert ME, McElrone AJ, Brodersen CR (2017) Excess Diffuse Light Absorption in Upper Mesophyll Limits CO₂ Drawdown and Depresses Photosynthesis. *Plant Physiol* 174(2):1082–1096. doi:10.1104/pp.17.00223
2. Bialasek M, Gorecka M, Mittler R, Karpinski S (2017) Evidence for the Involvement of Electrical, Calcium and ROS Signaling in the Systemic Regulation of Non-Photochemical Quenching and Photosynthesis. *Plant Cell Physiol* 58(2):207–215. doi:10.1093/pcp/pcw232
3. Acebron K, Matsubara S, Jedmowski C, Emin D, Muller O, Rascher U (2020) Diurnal dynamics of nonphotochemical quenching in *Arabidopsis* npq mutants assessed by solar-induced fluorescence and reflectance measurements in the field. *New Phytol.* doi:10.1111/nph.16984
4. Ikeuchi M, Sato F, Endo T (2016) Allocation of Absorbed Light Energy in Photosystem II in NPQ Mutants of *Arabidopsis*. *Plant Cell Physiol* 57(7):1484–1494. doi:10.1093/pcp/pcw072

5. Johnson MP, Perez-Bueno ML, Zia A, Horton P, Ruban AV (2009) The zeaxanthin-independent and zeaxanthin-dependent qE components of nonphotochemical quenching involve common conformational changes within the photosystem II antenna in Arabidopsis. *Plant Physiol* 149(2):1061–1075. doi:10.1104/pp.108.129957
6. Leunenberger M, Morris JM, Chan AM, Leonelli L, Niyogi KK, Fleming GR (2017) Dissecting and modeling zeaxanthin- and lutein-dependent nonphotochemical quenching in Arabidopsis thaliana. *Proc Natl Acad Sci U S A* 114(33):E7009–E7017. doi:10.1073/pnas.1704502114
7. Sacharz J, Giovagnetti V, Ungerer P, Mastroianni G, Ruban AV (2017) The xanthophyll cycle affects reversible interactions between PsbS and light-harvesting complex II to control non-photochemical quenching. *Nat Plants* 3:16225. doi:10.1038/nplants.2016.225
8. Kress E, Jahns P (2017) The Dynamics of Energy Dissipation and Xanthophyll Conversion in Arabidopsis Indicate an Indirect Photoprotective Role of Zeaxanthin in Slowly Inducible and Relaxing Components of Non-photochemical Quenching of Excitation Energy. *Front Plant Sci* 8:2094. doi:10.3389/fpls.2017.02094
9. Cazzaniga S, Dall' Osto L, Kong SG, Wada M, Bassi R (2013) Interaction between avoidance of photon absorption, excess energy dissipation and zeaxanthin synthesis against photooxidative stress in Arabidopsis. *Plant J* 76(4):568–579. doi:10.1111/tpj.12314
10. Tietz S, Hall CC, Cruz JA, Kramer DM (2017) NPQ(T): a chlorophyll fluorescence parameter for rapid estimation and imaging of non-photochemical quenching of excitons in photosystem-II-associated antenna complexes. *Plant Cell Environ* 40(8):1243–1255. doi:10.1111/pce.12924
11. Poudyal RS, Rodionova MV, Kim H, Lee S, Do E, Allakhverdiev SI, Nam HG, Hwang D, Kim Y (2020) Combinatory actions of CP29 phosphorylation by STN7 and stability regulate leaf age-dependent disassembly of photosynthetic complexes. *Sci Rep* 10(1):10267. doi:10.1038/s41598-020-67213-0
12. Brooks MD, Sylak-Glassman EJ, Fleming GR, Niyogi KK (2013) A thioredoxin-like/beta-propeller protein maintains the efficiency of light harvesting in Arabidopsis. *Proc Natl Acad Sci U S A* 110(29):E2733–E2740. doi:10.1073/pnas.1305443110
13. Roach T, Na CS, Stoggl W, Krieger-Liszakay A (2020) The non-photochemical quenching protein LHCSR3 prevents oxygen-dependent photoinhibition in *Chlamydomonas reinhardtii*. *J Exp Bot* 71(9):2650–2660. doi:10.1093/jxb/eraa022
14. Wilson S, Ruban AV (2020) Rethinking the Influence of Chloroplast Movements on Non-photochemical Quenching and Photoprotection. *Plant Physiol* 183(3):1213–1223. doi:10.1104/pp.20.00549
15. Liu J, Last RL (2017) A chloroplast thylakoid lumen protein is required for proper photosynthetic acclimation of plants under fluctuating light environments. *Proc Natl Acad Sci U S A* 114(38):E8110–E8117. doi:10.1073/pnas.1712206114
16. Sun X, Peng L, Guo J, Chi W, Ma J, Lu C, Zhang L (2007) Formation of DEG5 and DEG8 complexes and their involvement in the degradation of photodamaged photosystem II reaction center D1 protein in Arabidopsis. *Plant Cell* 19(4):1347–1361. doi:10.1105/tpc.106.049510

17. Liu H, Weisman D, Tang L, Tan L, Zhang WK, Wang ZH, Huang YH, Lin WX, Liu XM, Colon-Carmona A (2015) Stress signaling in response to polycyclic aromatic hydrocarbon exposure in *Arabidopsis thaliana* involves a nucleoside diphosphate kinase, NDPK-3. *Planta* 241(1):95–107. doi:10.1007/s00425-014-2161-8
18. Jarvi S, Isojarvi J, Kangasjarvi S, Salojarvi J, Mamedov F, Suorsa M, Aro EM (2016) Photosystem II Repair and Plant Immunity: Lessons Learned from *Arabidopsis* Mutant Lacking the THYLAKOID LUMEN PROTEIN 18.3. *Front Plant Sci* 7:405. doi:10.3389/fpls.2016.00405
19. Davletshina LN, Semin BK (2020) pH dependence of photosystem II photoinhibition: relationship with structural transition of oxygen-evolving complex at the pH of thylakoid lumen. *Photosynth Res* 145(2):135–143. doi:10.1007/s11120-020-00769-0
20. Motohashi K, Hisabori T (2006) HCF164 receives reducing equivalents from stromal thioredoxin across the thylakoid membrane and mediates reduction of target proteins in the thylakoid lumen. *J Biol Chem* 281(46):35039–35047. doi:10.1074/jbc.M605938200
21. Malnoe A, Schultink A, Shahrasbi S, Rumeau D, Havaux M, Niyogi KK (2018) The Plastid Lipocalin LCNP Is Required for Sustained Photoprotective Energy Dissipation in *Arabidopsis*. *Plant Cell* 30(1):196–208. doi:10.1105/tpc.17.00536
22. Bru P, Nanda S, Malnoe A (2020) A Genetic Screen to Identify New Molecular Players Involved in Photoprotection qH in *Arabidopsis thaliana*. *Plants (Basel)* 9 (11). doi:10.3390/plants9111565
23. Amstutz CL, Fristedt R, Schultink A, Merchant SS, Niyogi KK, Malnoe A (2020) An atypical short-chain dehydrogenase-reductase functions in the relaxation of photoprotective qH in *Arabidopsis*. *Nat Plants* 6(2):154–166. doi:10.1038/s41477-020-0591-9
24. Onoa B, Schneider AR, Brooks MD, Grob P, Nogales E, Geissler PL, Niyogi KK, Bustamante C (2014) Atomic force microscopy of photosystem II and its unit cell clustering quantitatively delineate the mesoscale variability in *Arabidopsis* thylakoids. *PLoS One* 9(7):e101470. doi:10.1371/journal.pone.0101470
25. Guinea Diaz M, Nikkanen L, Himanen K, Toivola J, Rintamaki E (2020) Two chloroplast thioredoxin systems differentially modulate photosynthesis in *Arabidopsis* depending on light intensity and leaf age. *Plant J* 104(3):718–734. doi:10.1111/tpj.14959
26. Hu F, Kang Z, Qiu S, Wang Y, Qin F, Yue C, Huang J, Wang G (2012) Overexpression of OsTLP27 in rice improves chloroplast function and photochemical efficiency. *Plant Sci* 195:125–134. doi:10.1016/j.plantsci.2012.06.006
27. Punchkhon C, Plaimas K, Buaboocha T, Siangliw JL, Toojinda T, Comai L, De Diego N, Spichal L, Chadchawan S (2020) Drought-Tolerance Gene Identification Using Genome Comparison and Co-Expression Network Analysis of Chromosome Substitution Lines in Rice. *Genes (Basel)* 11 (10). doi:10.3390/genes11101197
28. Jung YJ, Lee HJ, Yu J, Bae S, Cho YG, Kang KK (2020) Transcriptomic and physiological analysis of OsCAO1 knockout lines using the CRISPR/Cas9 system in rice. *Plant Cell Rep.* doi:10.1007/s00299-020-02607-y

29. Kim YA, Moon H, Park CJ (2019) CRISPR/Cas9-targeted mutagenesis of Os8N3 in rice to confer resistance to *Xanthomonas oryzae* pv. *oryzae*. *Rice (N Y)* 12(1):67. doi:10.1186/s12284-019-0325-7
30. Kang ZH, Huang JL, Zou HY, Zang GC, Wang GX (2015) Localization of OsTLP27 in thylakoid lumen is required for accumulation of photosynthetic proteins in rice. *Mol Breed* 35(7):9. doi:10.1007/s11032-015-0338-x
31. Hartings S, Paradies S, Karnuth B, Eisfeld S, Mehning J, Wolff C, Levey T, Westhoff P, Meierhoff K (2017) The DnaJ-Like Zinc-Finger Protein HCF222 Is Required for Thylakoid Membrane Biogenesis in Plants. *Plant Physiol* 174(3):1807–1824. doi:10.1104/pp.17.00401
32. Wang N, Zhang Y, Huang S, Liu Z, Li C, Feng H (2020) Defect in Brnym1, a magnesium-dechelate protein, causes a stay-green phenotype in an EMS-mutagenized Chinese cabbage (*Brassica campestris* L. ssp. *pekinensis*) line. *Hortic Res* 7:8. doi:10.1038/s41438-019-0223-6
33. Shin D, Lee S, Kim TH, Lee JH, Park J, Lee J, Lee JY, Cho LH, Choi JY, Lee W, Park JH, Lee DW, Ito H, Kim DH, Tanaka A, Cho JH, Song YC, Hwang D, Purugganan MD, Jeon JS, An G, Nam HG (2020) Natural variations at the Stay-Green gene promoter control lifespan and yield in rice cultivars. *Nat Commun* 11(1):2819. doi:10.1038/s41467-020-16573-2
34. Yamatani H, Kohzuma K, Nakano M, Takami T, Kato Y, Hayashi Y, Monden Y, Okumoto Y, Abe T, Kumamaru T, Tanaka A, Sakamoto W, Kusaba M (2018) Impairment of Lhca4, a subunit of LHCl, causes high accumulation of chlorophyll and the stay-green phenotype in rice. *J Exp Bot* 69(5):1027–1035. doi:10.1093/jxb/erx468
35. Simionato D, Basso S, Zaffagnini M, Lana T, Marzotto F, Trost P, Morosinotto T (2015) Protein redox regulation in the thylakoid lumen: the importance of disulfide bonds for violaxanthin de-epoxidase. *FEBS Lett* 589(8):919–923. doi:10.1016/j.febslet.2015.02.033
36. Kang ZH, Wang GX (2016) Redox regulation in the thylakoid lumen. *J Plant Physiol* 192:28–37. doi:10.1016/j.jplph.2015.12.012
37. Meyer AJ, Riemer J, Rouhier N (2019) Oxidative protein folding: state-of-the-art and current avenues of research in plants. *New Phytol* 221(3):1230–1246. doi:10.1111/nph.15436
38. Boca S, Koestler F, Ksas B, Chevalier A, Leymarie J, Fekete A, Mueller MJ, Havaux M (2014) Arabidopsis lipocalins AtCHL and AtTIL have distinct but overlapping functions essential for lipid protection and seed longevity. *Plant Cell Environ* 37(2):368–381. doi:10.1111/pce.12159
39. Ilik P, Spundova M, Sicner M, Melkovicova H, Kucerova Z, Krchnak P, Furst T, Vecerova K, Panzarova K, Benediktyova Z, Trtilek M (2018) Estimating heat tolerance of plants by ion leakage: a new method based on gradual heating. *New Phytol* 218(3):1278–1287. doi:10.1111/nph.15097
40. Wientjes E, Philippi J, Borst JW, van Amerongen H (2017) Imaging the Photosystem I/Photosystem II chlorophyll ratio inside the leaf. *Biochim Biophys Acta Bioenerg* 1858(3):259–265. doi:10.1016/j.bbabi.2017.01.008
41. Vilfan N, van der Tol C, Verhoef W (2019) Estimating photosynthetic capacity from leaf reflectance and Chl fluorescence by coupling radiative transfer to a model for photosynthesis. *New Phytol* 223(1):487–500. doi:10.1111/nph.15782

42. McClain AM, Sharkey TD (2020) Building a better equation for electron transport estimated from Chl fluorescence: accounting for nonphotosynthetic light absorption. *New Phytol* 225(2):604–608. doi:10.1111/nph.16255
43. Ptushenko VV, Zhigalova TV, Avercheva OV, Tikhonov AN (2019) Three phases of energy-dependent induction of [Formula: see text] and Chl a fluorescence in *Tradescantia fluminensis* leaves. *Photosynth Res* 139(1–3):509–522. doi:10.1007/s11120-018-0494-z
44. Steen CJ, Morris JM, Short AH, Niyogi KK, Fleming GR (2020) Complex Roles of PsbS and Xanthophylls in the Regulation of Nonphotochemical Quenching in *Arabidopsis thaliana* under Fluctuating Light. *J Phys Chem B* 124(46):10311–10325. doi:10.1021/acs.jpccb.0c06265
45. Belyaeva NE, Bulychev AA, Riznichenko GY, Rubin AB (2016) Thylakoid membrane model of the Chl a fluorescence transient and P700 induction kinetics in plant leaves. *Photosynth Res* 130(1–3):491–515. doi:10.1007/s11120-016-0289-z
46. Evans JR, Morgan PB, von Caemmerer S (2017) Light Quality Affects Chloroplast Electron Transport Rates Estimated from Chl Fluorescence Measurements. *Plant Cell Physiol* 58(10):1652–1660. doi:10.1093/pcp/pcx103
47. Gu L, Han J, Wood JD, Chang CY, Sun Y (2019) Sun-induced Chl fluorescence and its importance for biophysical modeling of photosynthesis based on light reactions. *New Phytol* 223(3):1179–1191. doi:10.1111/nph.15796
48. Liu Z, Wang Z, Gu H, You J, Hu M, Zhang Y, Zhu Z, Wang Y, Liu S, Chen L, Liu X, Tian Y, Zhou S, Jiang L, Liu L, Wan J (2018) Identification and Phenotypic Characterization of ZEBRA LEAF16 Encoding a beta-Hydroxyacyl-ACP Dehydratase in Rice. *Front Plant Sci* 9:782. doi:10.3389/fpls.2018.00782

Figures

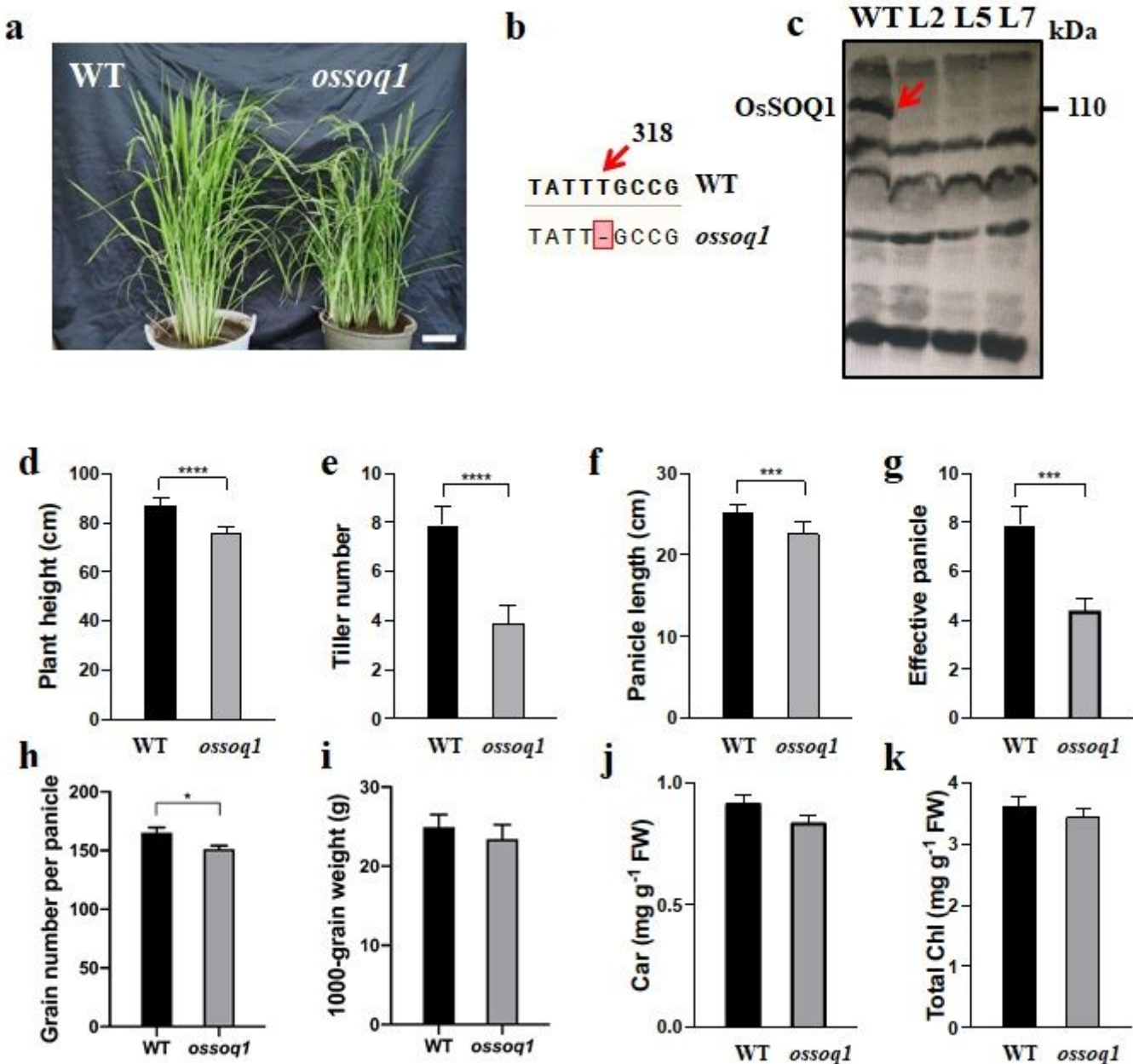


Figure 1

Positive identification, phenotype of transgenic plants and agronomic traits, and pigments comparison analysis of wild-type and transgenic plants. (a) Phenotype of wild-type and mutant plants were grown in soil until heading stage. Two lines for WT, and three (L2, L5 and L7) for mutant *ossoq1* were cultivated. Left: WT; right: *ossoq1*. Bar=10 cm. (b) The positive homogeneous plants were verified by sequencing; Snapgene software was used to align the DNA sequences. There was a T-deletion at position 381. Upper: WT; lower: *ossoq1*. (c) Western blot analysis of SOQ1 protein in wild-type and transgenic plants. Three mutant lines were used in this experiment. The molecular weight (MW) of OsSOQ1 (red asterisk) in WT is around 110 kDa, protein marker is listed on the right. Left: WT; right: L2, L5, L7. (d) Plant height (cm). (e) Panicle length (cm). (f) Tiller number. (g) Effective panicle number. (h) Grain number per panicle. (i) 1000-grain weight. (j) Total Car content. (k) Total Chl content. Error bars indicate standard deviation (+SD) and

representative data from three independent experiments are presented. For agronomic traits, twenty separate lines of wild-type and mutant were used. For pigments, six biological replicates was conducted. *: significant difference at $P < 0.05$ by Student's t-test; **: significant difference at $P < 0.01$ by Student's t-test. ***: significant difference at $P < 0.005$ by Student's t-test. ****: significant difference at $P < 0.001$ by Student's t-test.

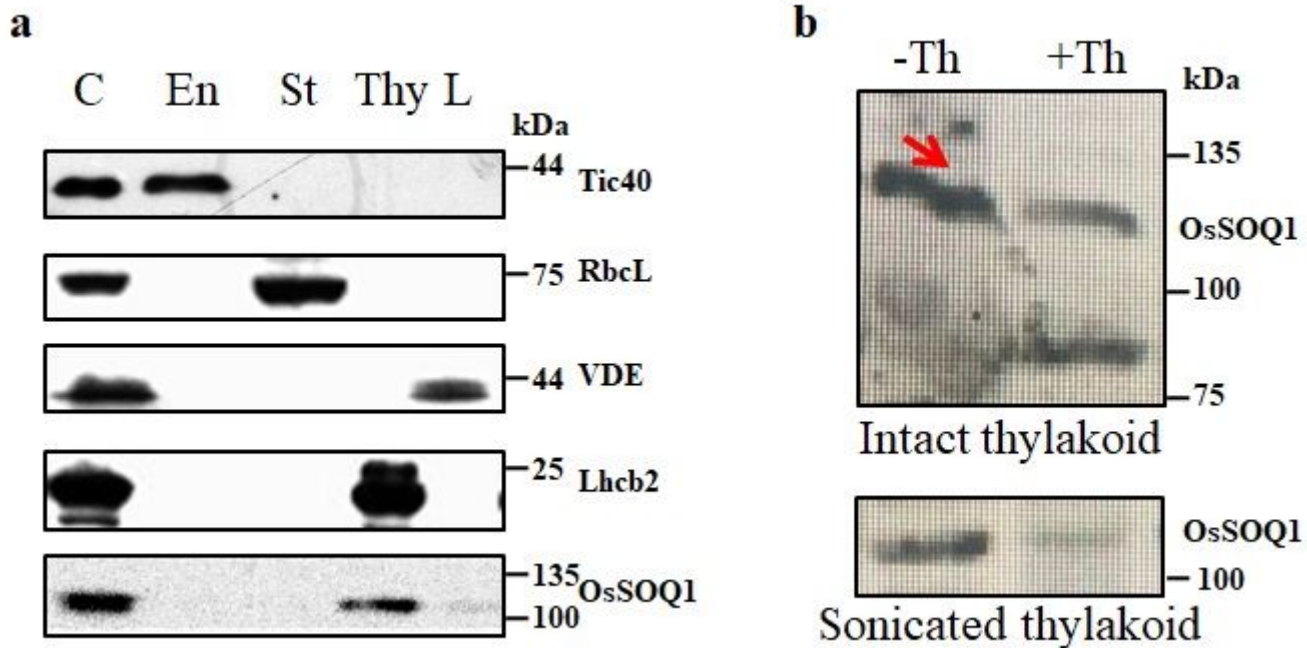


Figure 2

Subcellular and organelle subfraction localization of OsSOQ1. (a) Localization of OsSOQ1 in four compartments of Chloroplast, including envelope, stroma, thylakoid membrane and lumen. Tic40, RbcL, Lhcb2, and VDE are compartment markers for chloroplast envelope (En), stroma (St), thylakoid membrane (Thy) and lumen (L) respectively. Anti-OsSOQ1 antibody was used to detect the localization of OsSOQ1. Intact chloroplasts (C) were utilized as a positive control. (b) Orientation of the Trx-like domain in the thylakoid membrane. The intact and sonicated thylakoid membrane was treated with thermolysin (Th) ($20 \mu\text{g } \mu\text{L}^{-1}$) for 10 min, and the membrane samples was subjected into SDS-PAGE and immunoblotted with specific Anti-OsSOQ1 antibody.

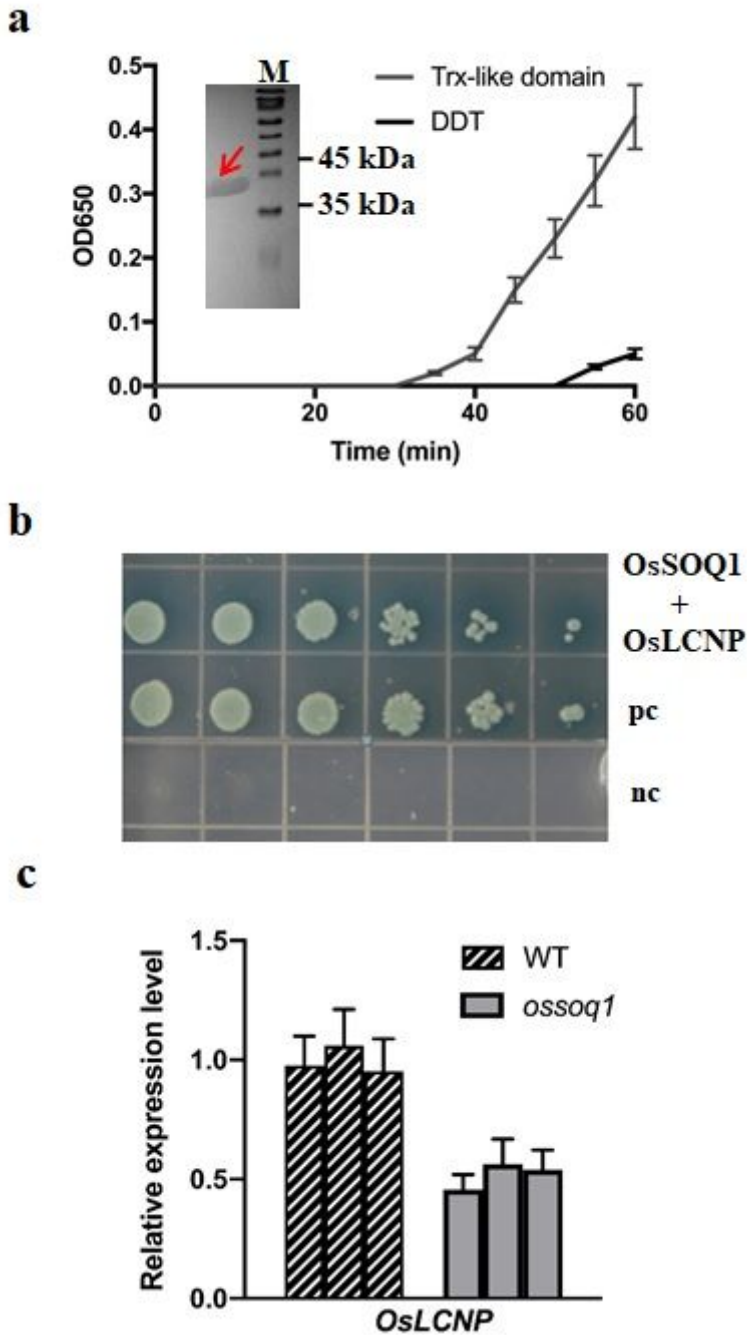


Figure 3

Expression pattern of OsSOQ1 under stress conditions, at different stages and in varying tissues, immuno-detection of photosynthetic proteins and Chl fluorescence in WT and mutant plants. Twenty micrograms of total protein was separated by SDS-PAGE and transferred to PVDF membrane, specific antibodies to OspsbC (CP43 protein of PSII), OspetB (cytochrome b6), ATP synthase, RbcL, RbcS, PsbS and VDE were used to detect individual protein. (a) Protein expression of OsSOQ1 induced by high light intensity (HL), cold (Co) and drought (Dr) stresses in CK and WT. (b) Protein expression of OsSOQ1 in leaves of 15-d-old (15 d), 8-week-old (8 w) and 15-week-old (15 w) WT plants. (c) Protein expression of OsSOQ1 in the stem (S), leaf blade (LB), leaf sheaths (LS) and young glume (YG) at heading stage. (d)

The maximum photochemical efficiency of PSII (Fv/Fm) in WT and *ossoq1*. (e) Protein level of *OspcbC* (CP43 of PSII), *OspetB* (cytochrome b6), ATP synthase, *RbcL*, and *RbcS* in WT and mutant plants under normal growth conditions. (f) Time-course of NPQ induction and relaxation in WT and mutant plants exposed to actinic light ($1200 \mu\text{mol m}^{-2} \text{s}^{-1}$). Prior to measurement, plants were dark-adapted for 20 min. (g) Protein level of *PsbS* and *VDE* in WT and mutant plants under normal growth conditions. For NPQ induction, three biological replicates were performed. Datas are means \pm SD (n=3). Anti-Actin is used as a loading control.

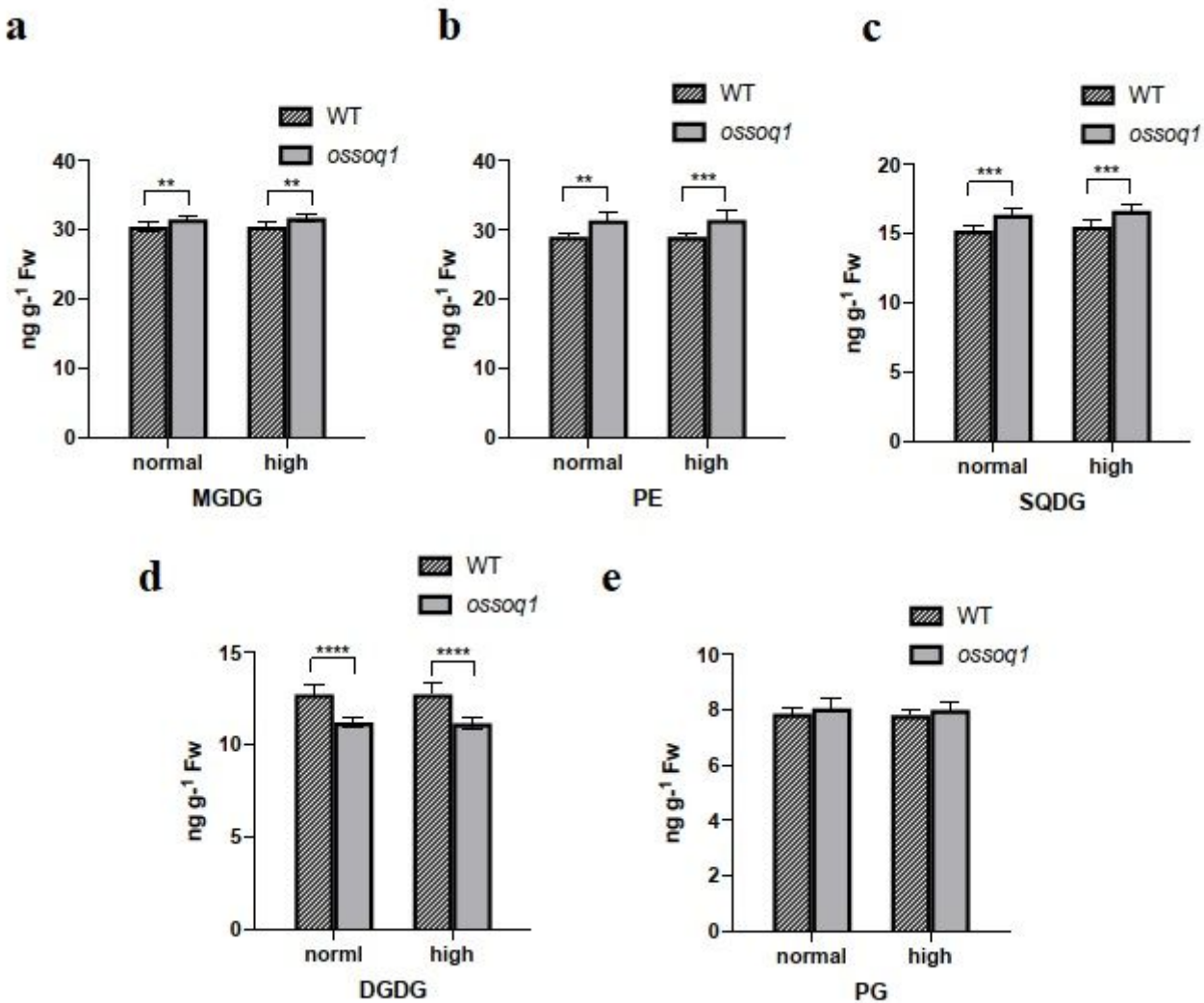


Figure 4

Reduction activity of Trx-like domain and interacting protein analysis. (a) Recombinant Trx-like domain protein was purified (red arrowhead), with a MW between 35 kDa and 45 kDa (in box). In vitro insulin assay was conducted for recombinant Trx-like domain protein. Five micromole of recombinant protein was used for activity analysis. DDT was used as a control. M, marker. (b) Yeast co-transformation of *OsSOQ1* and *OsLCNP* in vitro. The Trx-like domain of *OsSOQ1* was inserted into the vector pGBKT7 plasmid and transformed to yeast Y2H gold component cells, while *OsLCNP* was ligated in pGADT7 vector and transformed into yeast Y187 strain, then the two-hybrid strains were spread on QDO/X/A agar

with a ratio of 105:104:103:102:10:1. The colonies indicated positive reaction. Positive control: Y2Hgold (pGBKT7-53) and Y187 (pGADT7-T); Negative control: Y2Hgold (pGBKT7-Lam) and Y187 (pGADT7-T). pc, positive control; nc, negative control. (c) Total RNA was extracted from leaves of WT and mutant plants (L2, L5 and L7). Expression of OsLCNP of three mutant lines was analyzed by qRT-PCR. Error bars represent standard deviation (+SD) and representative data from three independent experiments are presented. **: significant difference at $P < 0.01$ by Student's t-test.

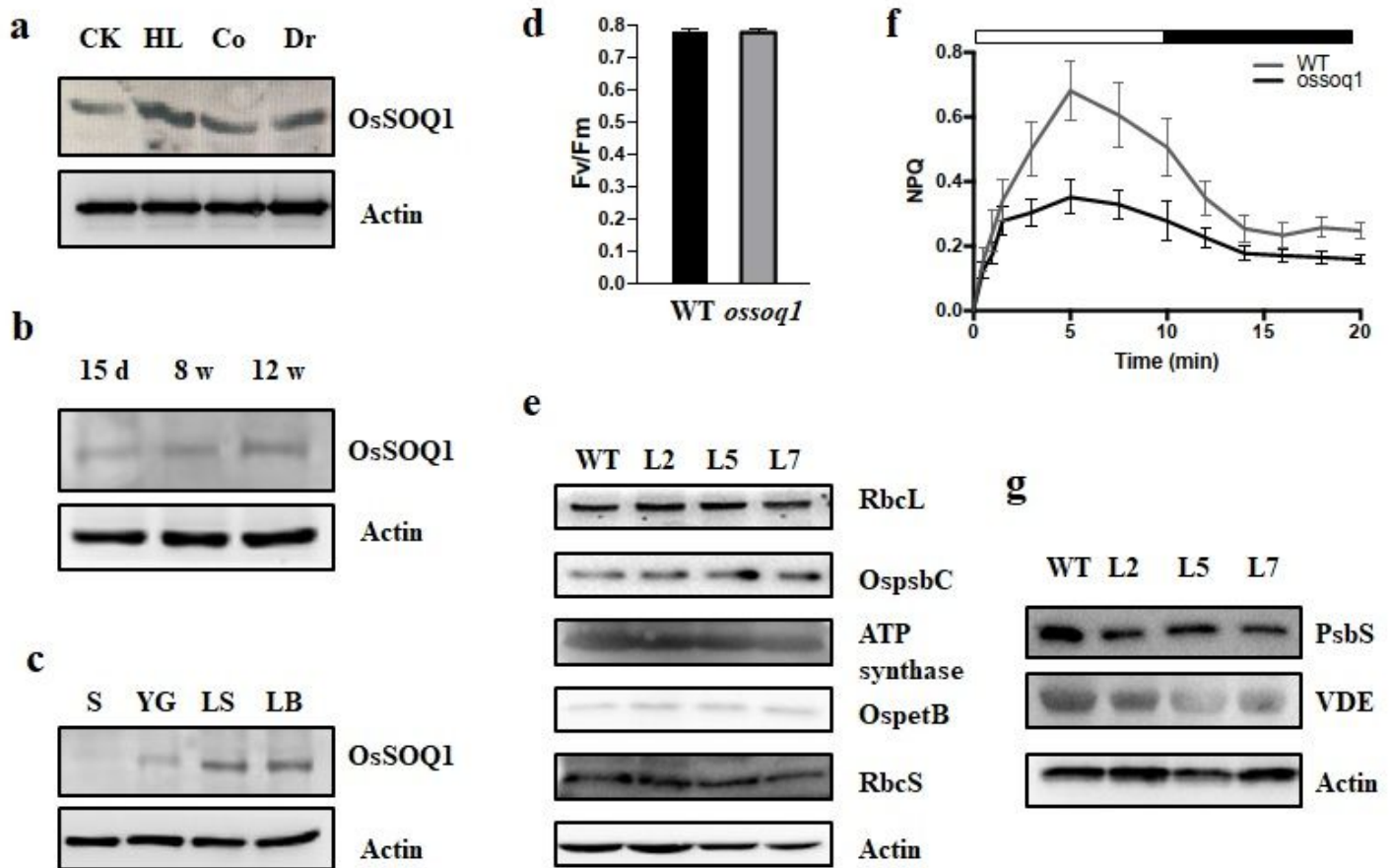


Figure 5

Thylakoid membrane lipids analysis of WT and *ossoq1* plants at tillering stage. Determination of fatty acids (polar lipid classes) by ELISA under normal growth and high light intensities for (a) monogalactosyl-diacylglycerol (MGDG); (b) digalactosyl-diacylglycerol (DGDG); (c) sulfoquinovosyldiacylglycerol (SQDG); (d) phosphatidylglycerol (PG); (e) phosphatidylethanolamine (PE). Datas are shown as means \pm SD ($n=6$).